

Refereed Proceedings

*The 12th International Conference on
Fluidization - New Horizons in Fluidization
Engineering*

Engineering Conferences International

Year 2007

X-Ray Fluoroscopy Measurements and
CFD Simulation of Hydrodynamics in a
Two Dimensional Gas-Solids Fluidized
Bed

Zhengxing He*

Bangyou Wu[†]

Blake Chandrasekaran[‡]

Celine Bellehumeur**

Apostolos Kantzas^{††}

*University of Calgary

[†]University of Calgary, bangyouwu@hotmail.com

[‡]University of Calgary

**University of Calgary, cbellehu@ucalgary.ca

^{††}University of Calgary, akantzas@ucalgary.ca

This paper is posted at ECI Digital Archives.

http://dc.engconfintl.org/fluidization_xii/58

He et al.: X-Ray Fluoroscopy Measurements and CFD Simulation

X-RAY FLUOROSCOPY MEASUREMENTS AND CFD SIMULATION OF HYDRODYNAMICS IN A TWO DIMENSIONAL GAS-SOLIDS FLUIDIZED BED

Zhengxing He^{1,2}, Bangyou Wu^{1,2}, Blake Chandrasekaran¹, Celine Bellehumeur²,
Apostolos Kantzas^{1,2}

¹Tomographic Imaging and Porous Media Laboratory

²Department of Chemical and Petroleum Engineering
Schulich School of Engineering

University of Calgary, Calgary, AB, Canada T2N 1N4

T: +1-403-220-8907; F: +1-403-282-5060; E: akantzas@ucalgary.ca

ABSTRACT

X-ray fluoroscopy measurements and CFD simulation were used to characterize the hydrodynamics in a pseudo 2-D gas-solids bubbling fluidized bed using polyethylene resin and glass beads. Bubble properties, such as bubble frequency, bubble size, bubble number distribution and bubble diameter distribution, were estimated from X-ray images and compared to those from CFD simulation.

INTRODUCTION

X-ray fluoroscopy, a non-intrusive imaging technique, can be used to characterize the hydrodynamics of fluidized beds. Substantial work on fluidization research using X-ray radiography has been performed by Rowe, Yates and co-workers at University College London since the 1960's, as reviewed by Yates et al (1). The effects of gas distributor, elevated temperatures and pressures, and co-axial nozzles on the dynamic properties of bubbles (growth, splitting, coalescence, velocity, wake and emulsion phase) have been studied via X-ray imaging. To date, however, most of the studies using the X-ray digital fluoroscopy have focused on the properties of single bubbles. Although some published studies did cover the bubbles of the full column, the column diameter is usually small (i.e. 10 cm). Can we get the bubble properties for wider beds? This work tries to solve this problem in a 2-D bed.

MFIX (Multiphase Flow with Interphase eXchanges), a general-purpose CFD code, was used to simulate the flow behavior under experimental conditions. Experimental results were used to verify the CFD predictions. By comparing the simulation results with experiments, CFD models and numerical methods can be verified so that they can be used to make improvements to the design and operation of fluidized bed reactors. Syamlal and O'Brien (2) simulated the laboratory-scale behavior of premixed O₃ decomposition in a bubbling fluidized bed using the multiphase CFD code MFIX. The grid-independent results were in very good agreement with reported experimental data for total conversion over a range of fluidization velocities and initial bed heights. The multiphase hydrodynamic models could quantitatively capture the effect of hydrodynamics on chemical reactions in the system studied. Hulme and

coworkers (3-5) used the multiphase CFD code Fluent to simulate 10 cm fluidized beds filled either with glass-beads or polyethylene particles. The simulated bubble properties agreed well with the results of X-ray fluoroscopy imaging experiments for the 10 cm diameter column. In this work, we considered gas-solids systems composed of either glass-beads or polyethylene powder particles, both particulate systems having comparable average particle size and narrow particle size distribution. Moreover, the flow behavior characteristics measured from X-ray fluoroscopy for each particulate system was compared to MFIX simulation.

EXPERIMENTAL

The fluidized bed system consisted of a pseudo 2-D bed made of Plexiglas with an inner width and thickness of 22.5 cm and 5 cm, respectively, the height of the fluidization section being 150 cm. A porous plate distributor was installed on the bottom of the column, and the gas entered the column through a cone at the bottom of an approximately 15 cm long chamber. The cone was filled with small plastic spheres (diameter=6.35 mm) and the chamber was empty to improve the gas distribution before reaching the distributor. Valves and rotameters were used to adjust and measure the gas flow rate, respectively.

Two types of particles were tested, glass-beads (GB) and polyethylene powder (PE). The column was filled with particles to a static bed height of 40 cm. Both particle systems had the similar mean particle size (360 μm) and particle size distribution (297 -420 μm), while they differed in density (2480 kg/m^3 for glass-beads and 924 kg/m^3 for polyethylene powder). It should be noted that the polyethylene resins are porous particles. The value of 924 kg/m^3 represents the plaque density and was used in determining the particle voidage. The particle density is 613 kg/m^3 (6). Both types of particles are classified as Geldart "B". The minimum fluidization velocity (U_{mf}) was determined by measuring the bed pressure at different velocities, and was found to be 11.0 cm/s for the glass-beads and 4.3 cm/s for the polyethylene powder. Three superficial gas velocities (U_g) were tested for each type of particles.

Four pressure transducers (Schlumberger Solartron, model 8000 DPD) were connected to column wall pressure ports located at a height $h=6, 16, 36,$ and 56 cm above the distributor using 0.32 cm nylon tubes. An A/D converter, a PC-LPM-16 card from National Instruments, and a personal computer were used for data acquisition. A self-developed Labview program records voltage data and stores them into the computer hard disc. The pressure data was collected at a rate of 500 Hz for 60 seconds at each flow rate. Each operating condition was sampled 20 times. Transducers were calibrated to establish the relationship of pressure versus voltage prior to the experimental measurements.

The X-ray fluoroscopy system (Figure 1) consisted of the X-ray tube, X-ray detector, image intensifier and image acquisition computer. The image acquisition system allowed to grab and store images at the rate of 30 frames per second. Calibration was performed using a series of phantom sets of known bulk density. Calibration curve of bulk density versus log value of grayscale number was obtained.

The effective diameter of the image was about 17 cm. The size of the image being less than the width of the column, the entire column was scanned by collecting images at six locations for every given superficial gas velocity. For each section of the column, approximately 2 minutes worth of images were collected which amounted to 3600 frames. A sample image is shown in Figure 2. Neighborhood averaging scheme was applied to the images to remove noise. A global threshold of grayscale number was used to determine the bubble boundary and binarize the grayscale images and a Matlab® program was written to identify and track bubbles. Additional details about the experimental setup and procedure can be found in reference (6).

He et al.: X-Ray Fluoroscopy Measurements and CFD Simulation

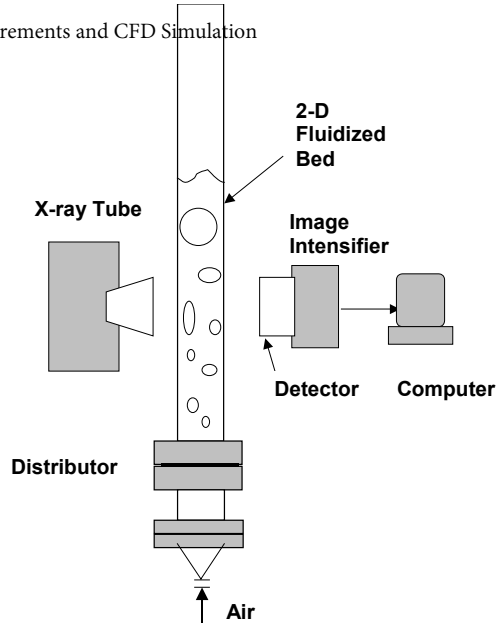


Figure 1. Schematic of the X-ray fluoroscopy setup

MFIX SIMULATION

The fluid dynamic models, equations, solved by MFIX code are based on an interpenetrating fluids formulation of multiphase flow (7). Due to the large content regarding MFIX code, it is not possible to provide a full description in this paper. For detailed information of equations and their applications, solution technique, simulation conditions, simulated bubble identification and tracking, reference (6, 8-9) and MFIX manuals (10) should be consulted. 2-D simulation in Cartesian coordinates was used in this study. The bed is assumed to be a rectangular plane with the front and back effect being neglected. For setting initial conditions, the bed was divided into two regions (bed and freeboard) with total height of 80cm. Both the static bed height and freeboard height are 40 cm. Table 1 lists the simulation conditions. Other conditions are the same as the experiments. A sample image is shown in Figure 3.

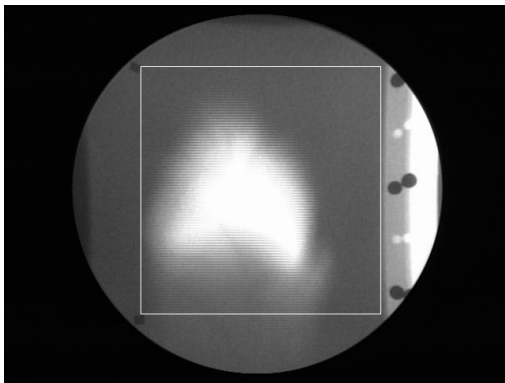


Figure 2. Raw image showing the circular field of view and the area of interest

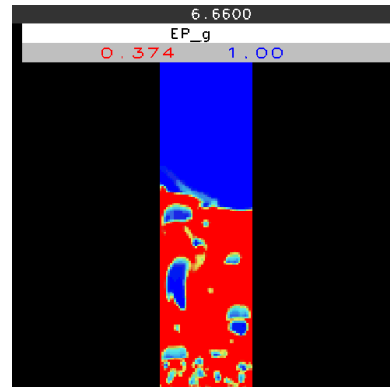


Figure 3. Sample image of the CFD simulation result

cropped for image processing
 The 12th International Conference on Fluidization - New Horizons in Fluidization Engineering, Art. 58 [2007]
 Table 1 Simulation Conditions

Boundary Condition	GB particle system	PE particle system
Outlet	Pressure	Pressure
Walls	No slip	No slip
Initial Condition	GB particle system	PE particle system
Minimum fluidization velocity (cm/s)	0.11	0.043
Initial Bed Voidage	0.374	0.356
Particle Property	GB	PE
Coefficient of Restitution	0.9	0.8
Angle of Internal Friction	30°	30°
Gas (Air) Property	GB particle system	PE particle system
Pressure (Pa)	101325	101325
Viscosity (kg/(m s))	1.7894e-4	1.7894e-4
Iteration	GB particle system	PE particle system
Time Step (s)	0.0001	0.0001
Stop Time of the Run (s)	32	32

RESULTS AND DISCUSSION

Grid independence studies were conducted previously by Chandrasekaran et al. (8-9) on a similar geometry. It was found that simulated average bubble diameter at different bed height (5-40cm) did not change significantly for square mesh size of 0.5cmX0.5cm and 0.3cmX0.3cm. In this work, square mesh size of 0.5cmX0.5cm was used. The bubble properties such as the diameter and velocities in this work are expected to be grid independent.

The pressure drop was obtained using average bed pressures. Syamlal and O'Brien (11) correlation was used for the drag model. The simulated pressure drop is higher than the experimental pressure drop, but the difference is less than 6% and 10% for GB and PE particles, respectively. From the work of McKeen and Pugsley (12), the drag law may need to be modified for particle like polyethylene resin due to the irregular shape and porous nature. The pressure drop decreases with an increase in the superficial gas velocity, as expected, which indicates an increase in voidage.

Figure 4 presents the average bubble diameter for experiment and simulation using the same method. It can be seen that there is an excellent agreement between the simulated and experimental bubble diameters at $2.5 U_{mf}$. Good agreement between simulation and experimental results was also obtained at other superficial gas velocities. Moreover, as the thickness of the 2D column used in this study is only 5 cm, bubble diameter close to or larger than 5 cm may be unstable due to the strong wall effect. Another observation from the results presented in Figure 4 is that, under comparable conditions, both experimentally measured and simulated bubble diameters for the GB system are larger than those for PE system. This difference in

the bubbling characteristics between GB and PE systems is likely due to the different particle properties: density, shape, and porosity. The formation of smaller bubbles in a gas-polyethylene fluidized bed can be seen as a beneficial feature, promoting a more uniform gas distribution which in turn would enhance mass and heat transfer, both very desirable in polymerization operations.

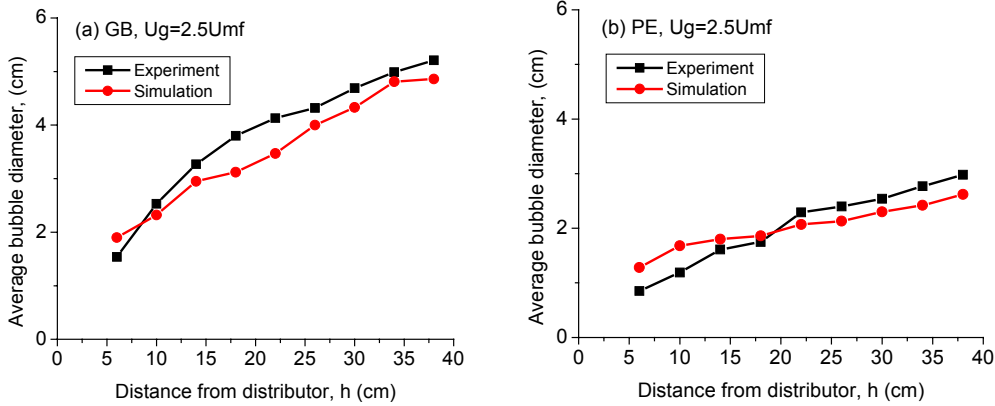


Figure 4. Average bubble diameters as a function of bed height at the superficial gas velocity of $2.5 U_{mf}$

Average vertical bubble velocities profiles at different U_g are shown in Figure 5. There are significant differences between the simulated and experimental vertical velocities. The lower experimental bubble velocities could be due to increased wall effects, which were not taken into consideration in the CFD simulations. Furthermore, experimental results also suggest that the vertical bubble velocity does not vary notably with variation of U_g , a behavior which was not captured by the CFD simulations. In general, CFD predicts slightly smaller bubble diameter (Figure 4), so in order to compensate for the same gas flow rate, bubble velocity must increase. Further work is in progress to explain the inconsistencies described above and improve agreement between experimental and simulation results.

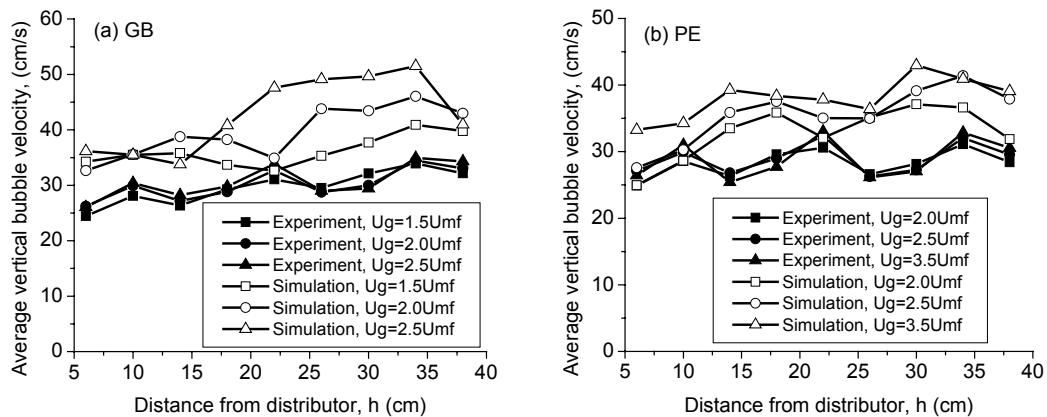


Figure 5. Average vertical bubble velocities as a function of bed height, filled symbols representing experimental results, empty symbols representing simulation results.

Figure 6 presents the average vertical bubble velocities as a function of bubble diameter. Results at other U_g are not shown in this paper, as they are similar to those obtained at $2.5 U_{mf}$. The simulated bubble velocities are higher than those from experiment. As we discussed above, substantial wall effects for 2-D bed in experiment could be the main reasons for these differences. Yet, the general trends of bubble velocity versus bubble diameter were similar for experimental and simulation. The simulation work needs to be improved, as the results are unstable, especially under high U_g for large bubbles.

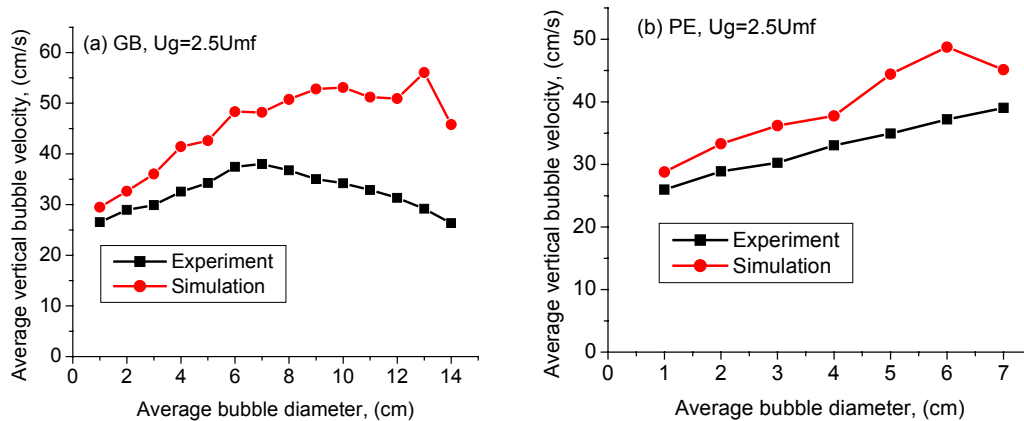


Figure 6. Average vertical bubble velocities as a function of bubble diameter at the superficial gas velocities of $2.5 U_{mf}$

Figure 7 shows the bubble number distribution profiles as a function of bed height. Simulation results do not match well with those from experiments, even though most of the general trends are similar. Possible reasons are limitation of the experimental method for accurate determination of small bubble number (especially for $h < 10\text{cm}$) and limitation of CFD simulation for PE particle system. At lower bed heights there is a possibility of missing smaller bubbles because of the averaging effect of the overall density, which could make detection of small bubbles nearly impossible. The different trends from simulation at lower bed heights for GB and PE systems needs to be further investigated.

Figure 8 shows a comparison of the experimental and simulated bubble size distributions at the superficial gas velocities of $2.5 U_{mf}$. It can be seen that both experiment and simulation have similar probability distributions except at small bubble diameters. Therefore, experimental measurement and CFD simulation for small bubbles should be further investigated. The high fraction of small bubbles for PE system from both experiments and simulation indicate uniform distribution of gas inside the reactor, which is an obvious advantage compared to GB system.

CONCLUSIONS

The bubbling characteristics of glass-beads and polyethylene powder systems were determined from X-ray fluoroscopy imaging. Our results suggest that the characteristics of polyethylene powder, which have a lower density, irregular shape and higher porosity compared to glass beads, greatly enhance the distribution of gas in the fluidization system. Experimental results were used to assess the validity of a MFIX code. While good agreement was obtained between the model predictions and

experimental results for the average bubble diameter. important discrepancies were seen for other bubbling characteristics. Further work is needed for both experiment, (e.g. small bubble detection) and simulations (e.g., drag law and wall effect in the model) in order to get more accurate hydrodynamic behavior in fluidized bed reactors for both GB and PE particles.

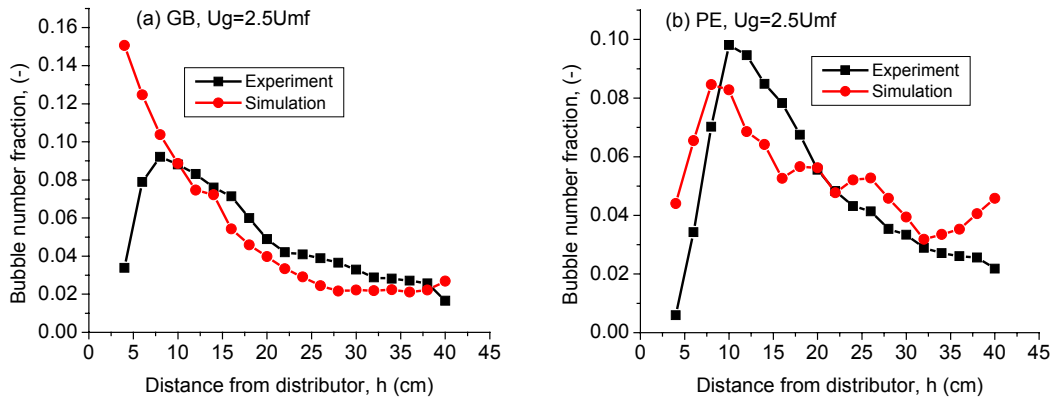


Figure 7. Bubble number distribution as a function of bed height at the superficial gas velocities of $2.5 U_{mf}$

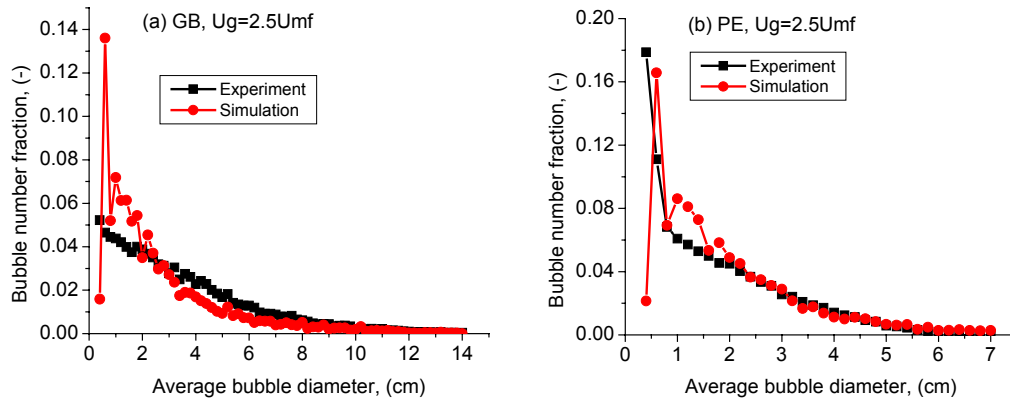


Figure 8. Bubble diameter distribution at the superficial gas velocities of $2.5 U_{mf}$

ACKNOWLEDGEMENTS

Financial support from the Natural Science and Engineering Research Council of Canada and the Canada Research Chairs Program is gratefully acknowledged.

NOTATION

- d_t column diameter [cm]
- h bed height from distributor [cm]
- U_g superficial gas velocity [cm/s]
- U_{mf} minimum fluidization velocity [cm/s]

REFERENCES

1. Yates, J. G., Cheesman, D.J., Lettieri, P. and Newton D. (2002). X-Ray Analysis of Fluidized Beds and Other Multiphase Systems. *KONA (Power Science and Technology in Japan)*, **20**, 133-143.
2. Syamlal, M. and O'Brien, T.J. (2003). Fluid Dynamic Simulation of O₃ Decomposition in a Bubbling Fluidized Bed, *AIChE J.*, **49** (11), 2793-2801.
3. Hulme, I., Clavelle, E., van der Lee, L., and Kantzas, A. (2005). CFD modeling and validation of bubble properties for a bubbling fluidized bed. *Ind. Eng. Chem. Res.* **44**, 4254-4266.
4. Hulme, I. and Kantzas, A. (2005). Validation of bubble properties of a bubbling fluidized bed reactor using CFD with imaging experiments. *Polymer-Plastics Tech. and Eng.* **44**, 73-95.
5. Hulme, I. and Kantzas, A. (2004). Determination of bubble diameter and axial velocity for a polyethylene fluidized bed using X-ray fluoroscopy. *Powder Techn.* **147**, 20-33.
6. He, Z.X., Comparison of the Behavior of Glass-beads and Polyethylene Resin Fluidized Beds Using X-ray Imaging Experiments and CFD Simulation, M.Sc. Thesis, University of Calgary, Calgary, Canada, 2005.
7. Anderson, T.B., and Jackson, R. (1967). A Fluid Mechanical Description of Fluidized beds, *Ind. Eng. Chem. Fundam.*, **6**, 527.
8. Chandrasekaran, B., van der Lee, L., Hulme, I. and Kantzas, A. (2005). A simulation and experimental study of the hydrodynamics of a bubbling fluidized bed of linear low density polyethylene using bubble properties and pressure fluctuations, *Macromolecular Material and Engineering*, **290**, 592-609.
9. Chandrasekaran, B., A Validation Study of the Computed Hydrodynamics of a Gas-Solid Fluidized Bed, MSc Thesis, University of Calgary, Calgary, Canada, 2004,
10. Syamlal, M., Rogers, W., and O'Brien, T.J. MFIx Documentation: Volume 1, Theory Guide, Technical Note: DOE/METC-94/1004, 1993.
11. Syamlal, M. and O'Brien, T. J. (1989), Computer simulation of bubbles in a fluidized bed, *AIChE Symposium Series*, **85** (270), 22-31.
12. McKeen, T. and Pugsley, T. (2003). Simulation and experimental validation of a freely bubbling bed of FCC catalyst. *Powder Techn.*, **129**, 139-152.